



Characteristics and possible mechanisms of diurnal variation of summertime precipitation in South Korea

Han-Gyul Jin¹ · Hyunho Lee² · Jong-Jin Baik¹

Received: 12 November 2021 / Accepted: 28 January 2022 / Published online: 4 February 2022
© The Author(s), under exclusive licence to Springer-Verlag GmbH Austria, part of Springer Nature 2022

Abstract

This study analyzes the characteristics of diurnal variation of precipitation in South Korea in June and July using 10-yr nationwide rain gauge data and investigates possible mechanisms for this. The diurnal variation of precipitation amount has two peaks, a primary peak at 05–08 LST and a secondary peak at 16–18 LST. Both the precipitation intensity and frequency contribute to each of the two peaks, but to the morning (late afternoon) peak, the contribution of precipitation intensity (frequency) is slightly larger. Spatially, afternoon-to-evening peaks (14–22 LST) appear in the mountainous regions and the south coastal region, and late night-to-morning peaks (02–10 LST) appear in the west and east coastal regions and the western inland regions. Rainy days are divided into days with late night-to-morning peaks (LNMP days) and days with afternoon-to-evening peaks (AEP days), which are associated with different mechanisms. The LNMP days are characterized by enhanced large-scale low-level southwesterlies toward South Korea and resultant large-scale and heavy precipitation, while the AEP days are characterized by relatively weak synoptic forcing for precipitation. On the LNMP days, the low pressure anomaly over the Yellow Sea in the late night and the nocturnal acceleration of low-level monsoonal southerlies driven by the boundary layer inertial oscillation cause the late night-to-morning precipitation peak. The radiative cooling at the cloud top and increased upper-level snow in the late night also contribute to the peak. On the AEP days, the destabilization of the low atmosphere due to daytime surface heating yields a higher chance of convective precipitation in the afternoon. Strong near-surface convergence in the afternoon over the mountainous regions due to sea breezes and upslope winds enhances afternoon precipitation. The downslope winds from the mountainous regions cause near-surface convergence over the inland region in the evening, contributing to evening precipitation.

1 Introduction

The rainy season brought by the East Asian summer monsoon mostly starts from mid-May to late May and ends from late July to early August in eastern China, the Korean Peninsula, and Japan (Qian et al. 2002). Because the precipitation in this season accounts for a great portion of the annual precipitation in East Asia, its spatiotemporal variations have drawn much attention. Among them, the diurnal variation of precipitation (DVP) has been found to be distinct in many regions in East Asia.

Since Ramage (1952) who analyzed the summertime DVP in East Asia, many studies have shown distinctive features of DVP in various regions in East Asia influenced by the great complexity of geography and the summer monsoon (Fujibe 1988; Oki and Musiake 1994; Lim and Kwon 1998; Yu et al. 2007; Yuan et al. 2012b). In China, diurnal precipitation peaks appear from the late afternoon to midnight in the Tibetan Plateau, from the midnight to early morning in the western China Plain, twice in the early morning and in the late afternoon in the eastern China Plain, and in the late afternoon in south and northeast China (Yu et al. 2007; Yuan et al. 2012b). In Japan, coastal regions tend to have morning peaks, while inland regions tend to have two peaks, one in the morning and the other in the evening (Oki and Musiake 1994).

In comparison with China and Japan, South Korea has a relatively small territory, but it exhibits substantial regional differences in DVPs within the country. In the study of Ramage (1952), South Korea was divided into three regions

✉ Hyunho Lee
hyunho.lee@kongju.ac.kr

¹ School of Earth and Environmental Sciences, Seoul National University, Seoul 08826, South Korea

² Department of Atmospheric Science, Kongju National University, Gongju 32588, South Korea

with different types of DVPs, which are the west coast with a significant morning maximum, a part of the east coast with no significant maximum but more afternoon precipitation than its surroundings, and the remainder of the country with a less significant morning maximum (plus a less significant afternoon maximum if inland). Lim and Kwon (1998) focused on the DVP in South Korea in the warm season using hourly precipitation data in the years 1980–1996. They stated that the DVP in South Korea can be characterized by two peaks in the early morning and in the afternoon and the relative magnitudes of the two peak values vary by region. The number of rain gauge points considered in Lim and Kwon (1998) was 31, and most of the mountainous regions were not covered, which makes it difficult to examine the strong spatial variability of DVPs within the country due to the complex geographical features. Jung et al. (2001) analyzed historical precipitation data in Seoul, South Korea. They showed that during historical wet periods, the amplitude of normalized diurnal variation was larger and the morning precipitation peak appeared earlier for heavy precipitation than for light and moderate precipitation.

The dense network of rain gauges nowadays in South Korea makes it possible to examine the strong spatial variability of DVP characteristics within the country. Satellite retrieval-based precipitation products have been tested for use in examining DVPs in several regions in East Asia, but they tend to underestimate morning precipitation and overestimate afternoon precipitation (Yuan et al. 2012a) or show diurnal variations of precipitation frequency and intensity that are too strong (Li et al. 2018). Therefore, based on the high-resolution rain gauge data, this study aims to describe the detailed characteristics of DVP in South Korea which have not been identified by previous studies.

In addition to the characteristics of DVP, the mechanisms associated with DVP deserves in-depth investigation. Few studies have been carried out to determine the reasons for the distinctive DVP in South Korea. Kim et al. (2010) examined the diurnal variation of precipitation in South Korea in June–August 2007 through Weather Research and Forecasting model simulations. They found that the DVP from 1 June to 21 July is dominated by nighttime precipitation and is associated with large-scale disturbances, while the DVP from 22 July to 31 August is dominated by daytime precipitation and is related to the local convective activity driven by thermal instability. Roh et al. (2012) analyzed the DVP in South Korea during the 2009 summer using the cyclostationary empirical orthogonal function analysis method. They related the southward migration of the precipitation band to the nighttime precipitation peak and the quasi-stationary precipitation over the north-central region of South Korea to the daytime precipitation peak. However, these features obtained from the studies using one-year data may not be representative enough to explain the general summertime DVP in South Korea. In addition, potential

mechanisms for DVP such as diurnal variability of monsoonal flow and local wind circulations, which have turned out to play important roles in DVPs in nearby regions (Chen 2020; Song and Zhang 2020), were not addressed. Therefore, a comprehensive study that examines a variety of possible mechanisms that explain the general characteristics of summertime DVP in South Korea is needed.

This study examines the characteristics of DVP in South Korea using nationwide rain gauge data, focusing on June and July when this country is dominated by the East Asian summer monsoon. Then, we seek the mechanisms that are responsible for the characteristic DVP in South Korea. Section 2 describes the datasets used in this study. Section 3 presents the results and discussion. In Section 4, a summary and conclusions are provided.

2 Datasets

The analysis period in this study is June–July of the years 2011–2020. The hourly rain gauge data in this period observed at 502 rain gauge points are provided by the Korea Meteorological Administration. The locations of the rain gauge points are shown in Fig. 3b. The 502 rain gauge points exclude the rain gauge points that have a non-negligible number of missing data (more than 3% of the total data) during the analysis period. Because the rain gauge's minimum measurable precipitation amount is 0.1 or 0.5 mm depending on the observation instrument, the hourly precipitation amounts smaller than 0.5 mm are regarded as 0 mm to use the data from both kinds of rain gauges having different minimum measurable precipitation amounts with consistency. This does not significantly affect the results in this study.

To examine the possible mechanisms for DVP, this study uses meteorological variables in the European Centre for Medium-Range Weather Forecasts Reanalysis version 5 (ERA5, Hersbach et al. 2020) data. The ERA5 data have a temporal resolution of 1 h and a spatial resolution of $0.25^\circ \times 0.25^\circ$, which have been utilized to investigate diurnal variations of atmospheric states (e.g., Huang et al. 2021). Throughout the study, only the local standard time of South Korea (UTC + 9 h) is used to represent time, although the meteorological fields analyzed in this study cover some regions with different time zones (UTC + 8–10 h) in East Asia.

3 Results and discussion

3.1 General characteristics of DVP in South Korea

In this subsection, the general characteristics of DVP in South Korea are given. The hourly precipitation amount

shows two peaks, one in the late night to morning and the other in the late afternoon (Fig. 1a). The hourly precipitation amount averaged over 05–08 LST in the higher peak is 25% larger than that averaged over 16–18 LST in the lower peak. Local minima of precipitation amount are observed at 13–14 LST and 22–23 LST. The relative frequency of precipitation occurrence also shows two peaks, the higher peak in the late night to morning and the lower peak in the afternoon, but the higher peak is relatively narrow compared to that of the precipitation amount (Fig. 1b). The precipitation intensity, that is, the precipitation rate averaged over non-zero values, shows a broad peak in the late night to morning and two local maxima at 14–15 LST and 16–17 LST (Fig. 1c), which precede the afternoon peak of the precipitation frequency.

The diurnal variations of precipitation frequency and intensity both contribute to the diurnal variation of precipitation amount. In this study, their relative contributions are investigated using the method of Li et al. (2013). The precipitation amount (PA) is the product of the number of precipitation occurrences (PO) and the precipitation intensity (PI). Taking a logarithm and applying a total differential, their relationship can be expressed as follows:

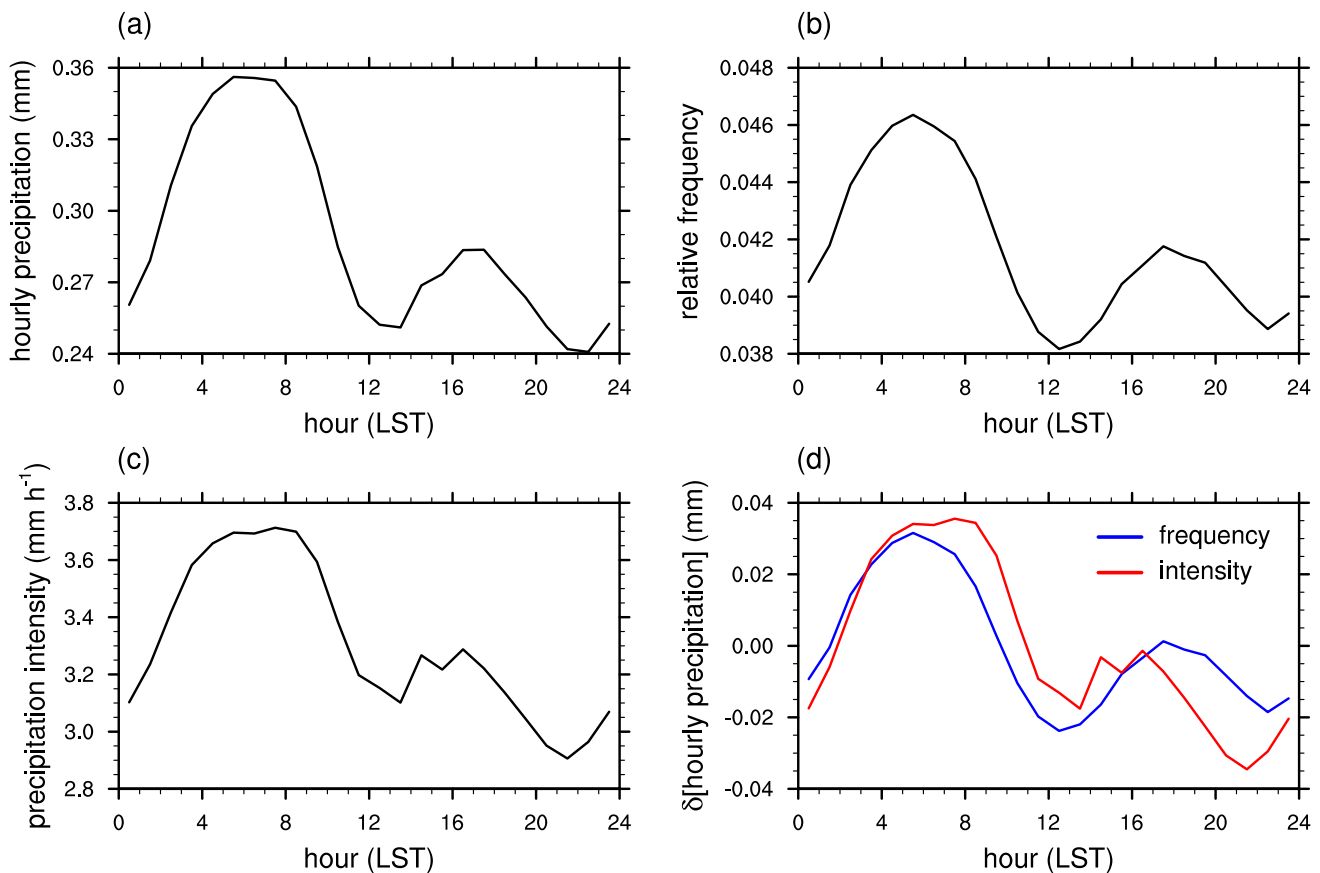


Fig. 1 Diurnal variations of (a) hourly precipitation amount, (b) relative frequency of precipitation occurrence, (c) precipitation intensity, and (d) contributions of precipitation frequency and intensity to the diurnal variation of precipitation amount

$$dPA = PI \times dPO + PO \times dPI \quad (1)$$

Integration of Eq. (1) from the daily mean to the value at a specific time with an assumption that the integrands are constant gives the following relationship:

$$\delta PA = \bar{PI} \times \delta PO + \bar{PO} \times \delta PI \quad (2)$$

where δ indicates the deviation of the value at a specific time from the daily mean and the bar indicates the daily mean. The first and second terms on the right-hand side of Eq. (2) represent the contributions of diurnal deviations of precipitation frequency and intensity to the diurnal deviation of precipitation amount, respectively. The sum of these two terms successfully represents the diurnal deviation of precipitation amount (not shown), implying that the approximation that has been made to obtain Eq. (2) does not cause a large error. Lim and Kwon (1998) stated that the diurnal variation of precipitation amount in South Korea is dominated by the precipitation frequency rather than the precipitation intensity by analyzing the diurnal maximum value of hourly precipitation for each day and its occurrence time, but the analysis

in this study using Eq. (2) gives a different result. Figure 1d shows that the answer for the question “which is the more important contributor?” changes diurnally. The morning peak of precipitation amount at 05–08 LST is caused by both the high precipitation frequency and high precipitation intensity, but the contribution of the precipitation intensity is larger. In contrast, the precipitation frequency contributes slightly more to the afternoon peak at 16–18 LST. For the local minimum of precipitation amount at 11–14 LST, the low precipitation frequency is mainly responsible. The diurnal minimum of precipitation amount at 21–23 LST is mainly caused by the low precipitation intensity.

Figure 2 shows the diurnal variations of precipitation amount for different precipitation intensity categories. Light precipitation ($0.5\text{--}2 \text{ mm h}^{-1}$) has the smallest amplitude of diurnal variation, and the afternoon peak appears at 18–19 LST, later than that of total precipitation. In comparison with light precipitation, moderate precipitation ($2\text{--}10 \text{ mm h}^{-1}$) has a larger diurnal variation amplitude. Heavy precipitation ($\geq 10 \text{ mm h}^{-1}$) has the largest diurnal variation amplitude, and the two peaks in the morning and afternoon are pronounced, indicating that heavy precipitation is most responsible for the bimodal structure of total DVP.

The complex geographical features of South Korea result in different patterns of DVP within the country. The spatial distribution of the peak time of precipitation amount is presented in Fig. 3a. In terms of the peak time of precipitation, the rain gauge points in South Korea are roughly divided into two groups, one with late night-to-morning peaks and the other with afternoon-to-evening peaks (Fig. 3c). Rain gauge points with peak times close to noon (10–14 LST) and midnight (22–02 LST) are rare. Interestingly, the rain gauge points with afternoon-to-evening (14–22 LST) peaks of precipitation are mainly located in the mountainous regions of the Taebaek Mountains and Sobaek Mountains (the locations of these regions are indicated in Fig. 3b) and in the region between them (east of the Sobaek Mountains).

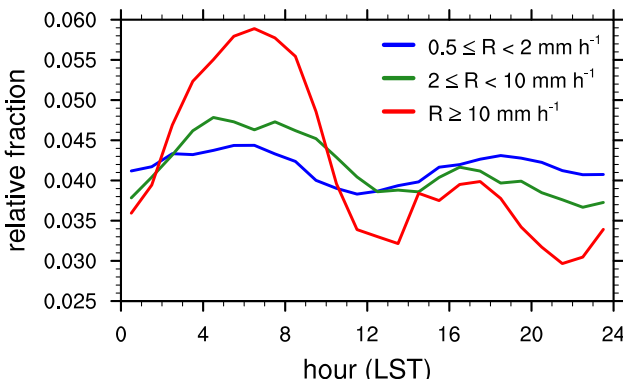


Fig. 2 Diurnal variations of relative fraction of hourly precipitation amount for different precipitation intensity categories

The afternoon-to-evening peaks are also found in the south coastal region of South Korea. It seems that the mountain–plains solenoid and sea breezes play some roles in the afternoon-to-evening peak of precipitation in these regions. The west and east coastal regions and the inland regions west of the mountainous regions mostly have late night-to-morning (02–10 LST) peaks of precipitation. Figure 3d shows that the rain gauge points with afternoon-to-evening peaks also receive a large amount of late night-to-morning precipitation, showing a clear bimodal structure of DVP. In contrast, the rain gauge points with late night-to-morning peaks receive a much smaller amount of precipitation in the afternoon to evening than in the late night to morning. If it is supposed that late night-to-morning precipitation and afternoon-to-evening precipitation are associated with different physical mechanisms, the above results imply that the dominant mechanisms for DVP are different from region to region within South Korea.

The peak time of precipitation varies temporally as well as spatially. The peak time of precipitation for each rainy day is obtained from the diurnal variations of precipitation averaged over all rain gauge points in South Korea. Here, a rainy day is defined as a day on which the daily precipitation amount averaged over all rain gauge points is greater than 0.1 mm. Within the June–July period analyzed in this study, the peak time does not have a noticeable intra-seasonal preference and changes considerably within a few days (not shown). Figure 4a shows the diurnal variation of daily precipitation amount according to peak time; the daily precipitation amounts of days with the same peak times are averaged. The days with late night-to-morning (02–10 LST) peaks of precipitation (hereafter LNMP days) account for 47% of the total precipitation amount, and the days with afternoon-to-evening (14–22 LST) peaks of precipitation (hereafter AEP days) account for 28% of the total precipitation amount. The LNMP days and AEP days account for 31% and 36% of the total number of rainy days, respectively. In comparison with the LNMP days, the AEP days are more frequent but have a smaller amount of precipitation. The DVPs on these two groups of rainy days are clearly distinguished from each other (Fig. 4b). Each group shows a single-peak and smooth DVP, contributing to each peak in the total DVP. This implies that the LNMP days and AEP days may have different meteorological conditions associated with precipitation and hence have different mechanisms for DVP. These are investigated in the following subsections.

3.2 LNMP days and AEP days

Figure 5 shows the spatial distributions of daily precipitation amount and the spatial distributions of the peak time of precipitation amount on the LNMP days and AEP days. The two groups of rainy days show clearly different spatial

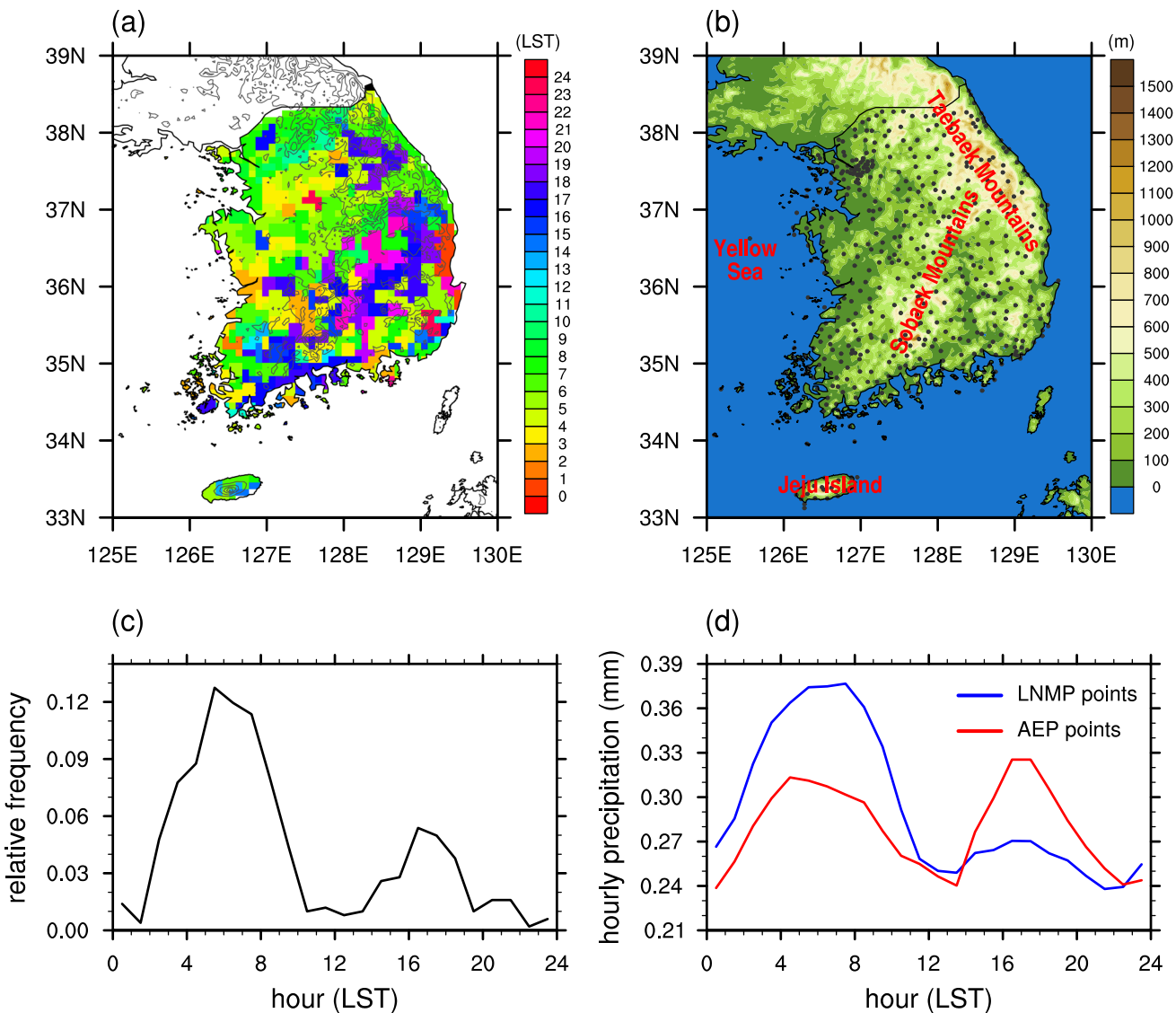


Fig. 3 (a) Peak time of diurnal variation of precipitation amount for each rain gauge point (color shades, LST) with topographic height (gray contours, in 300-m intervals) and (c) its relative frequency. (b) Topographic map of South Korea and surrounding regions with the locations of the 502 rain gauge points. (d) Diurnal variations of precipitation amount averaged over rain gauge points with late night-to-morning peaks (02–10 LST, blue solid line) and afternoon-to-evening peaks (14–22 LST, red solid line)

distributions of precipitation. On the LNMP days, precipitation mainly occurs in the northern and western parts of South Korea (Fig. 5a). On the AEP days, the southern part of South Korea, especially the Sobaek Mountains and Jeju Island ($\sim 33.2\text{--}33.6^\circ\text{N}$, $\sim 126.2\text{--}126.9^\circ\text{E}$), receives a large amount of precipitation, and the Taebaek Mountains and the northern inland region west of the Taebaek Mountains also receive relatively large amounts of precipitation compared to the west and east coastal regions (Fig. 5b). The spatial distributions of the peak time of precipitation amount on the LNMP days and AEP days are totally different from each other. On the LNMP days, most of the country shows late night-to-morning peaks of precipitation (Fig. 5c). In

contrast, most of the country shows afternoon-to-evening peaks of precipitation on the AEP days (Fig. 5d). There certainly exists some degree of spatial variability of peak time for each group of rainy days, but it is relatively very weak compared to that for all rainy days (Fig. 3a).

The different spatiotemporal distributions of precipitation on the LNMP days and AEP days are associated with different meteorological conditions. In summer, warm and moist air is transported to South Korea from the East China Sea by southwesterly monsoonal flows supported by the subtropical high over the northwestern Pacific Ocean (Fig. 6a and b). On the LNMP days, the subtropical high extends to the northwest (Fig. 6a). This increases the pressure gradient

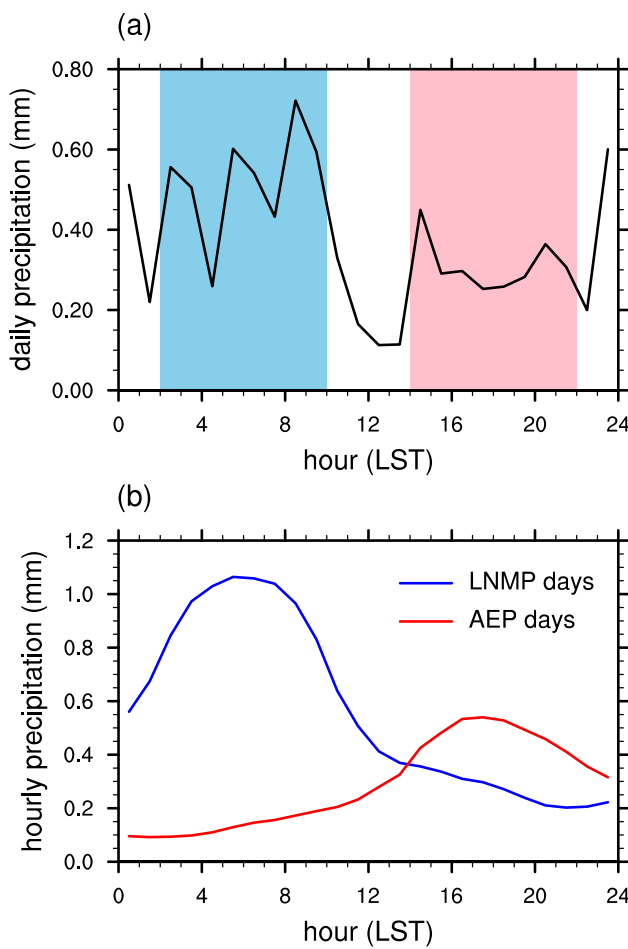


Fig. 4 (a) Diurnal variation of daily precipitation amount according to peak time. The daily precipitation amounts of days with the same peak times are averaged. The times of late night to morning (02–10 LST) and afternoon to evening (14–22 LST) are shaded in light blue and pink, respectively. (b) Diurnal variations of hourly precipitation amount averaged over the LNMP days and AEP days

over the northern part of the East China Sea and enhances the geostrophic southwesterlies toward South Korea. In addition, a low-level synoptic trough lies over the west of the Korean Peninsula, which is represented as a strong negative pressure anomaly centered at the west coast of the Korean Peninsula. As a result, a south–north contrast of warm/moist and cool/dry air appears over South Korea (Fig. 6c), which is regarded as the activation of the Changma front. These put South Korea into favorable conditions for large-scale and heavy precipitation. On the AEP days, the subtropical high extends to the southwest (Fig. 6b). This loosens the pressure gradient over the northern part of the East China Sea. A high pressure anomaly affects South Korea and produces easterly anomalies that blow against the mean southwesterlies (Fig. 6d). These provide South Korea with little chance of synoptically forced precipitation. The anomalous equivalent potential temperature field shows that the low atmosphere

over the western part of South Korea is more heated than that over surrounding seas, possibly due to the greater surface heating under relatively clear skies on the AEP days, which will be discussed in the next subsection.

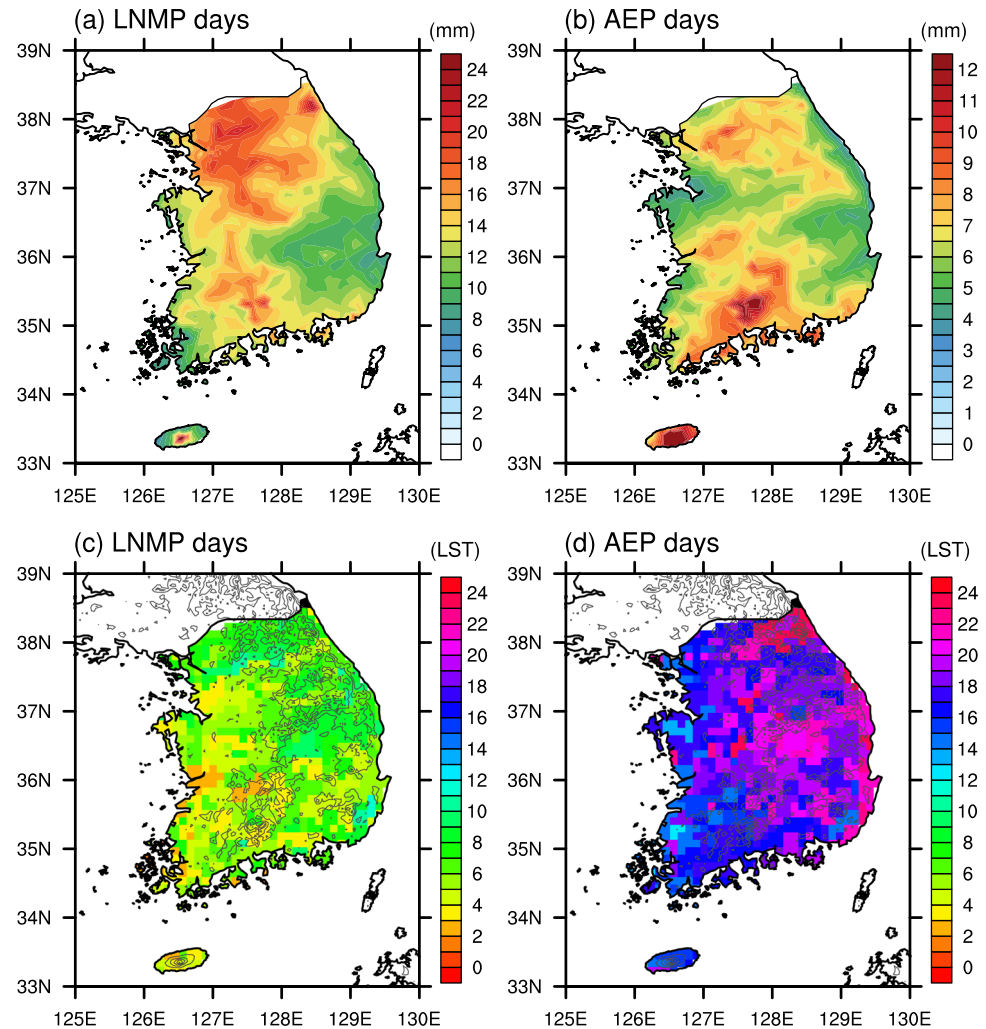
3.3 Possible mechanisms for DVP on the LNMP days and AEP days

In this subsection, possible mechanisms for DVP in South Korea are suggested by investigating the relationships between the DVP and the diurnal variations of meteorological variables in and around South Korea. Because the previous subsection shows that the two groups of rainy days, the LNMP days and AEP days, have clearly different characteristics of DVP and clearly different meteorological conditions, for each group the important mechanisms for its DVP are examined. The possible mechanisms are roughly divided into three categories: diurnal variations of synoptic-scale circulation, thermodynamic instability, and local wind circulation.

3.3.1 Diurnal variation of synoptic-scale circulation

The summertime precipitation in South Korea is dominated by synoptic-scale forcing, i.e., the East Asian summer monsoon, indicating that the diurnal evolutions of synoptic patterns and large-scale low-level flows can affect the DVP. Figure 7 shows the diurnal variation of anomalous synoptic pattern at 850 hPa on the LNMP days and AEP days. On the LNMP days, a low pressure anomaly lies over the east coast of China at 00 LST. It moves eastward with time and centers on the Yellow Sea (located between the east coast of China and the Korean Peninsula) at 03–06 LST, transporting warm and moist air from the southwest to South Korea and enhancing the Changma front. The pattern is reversed at 15 LST, that is, a high pressure anomaly and resultant anti-cyclonic circulation and divergence lie over the Yellow Sea. This weakens the southwesterly monsoonal flow during the afternoon and evening, suppressing the monsoonal precipitation during that time period. On the AEP days, the diurnal variation of low-level flows around South Korea is not as large as that on the LNMP days, indicating a smaller contribution of diurnal variation of synoptic-scale forcing to the DVP on the AEP days. In contrast to the LNMP days, the AEP days exhibit a high pressure anomaly over the Yellow Sea and the Korean Peninsula at 00–09 LST, which suppresses precipitation in the late night to morning and clears the sky so that a large amount of solar radiation reaches and heats the surface in the daytime. At 18–21 LST, a cyclonic circulation anomaly develops, centering slightly offshore of the west coast of the Korean Peninsula. To some extent, this contributes to the afternoon to evening peak of precipitation on the AEP days.

Fig. 5 Spatial distributions of daily precipitation amount averaged over the (a) LNMP days and (b) AEP days. Spatial distributions of peak time of diurnal variation of precipitation amount for each rain gauge point (color shades) on the (c) LNMP days and (d) AEP days with topographic height (gray contours, in 300-m intervals)

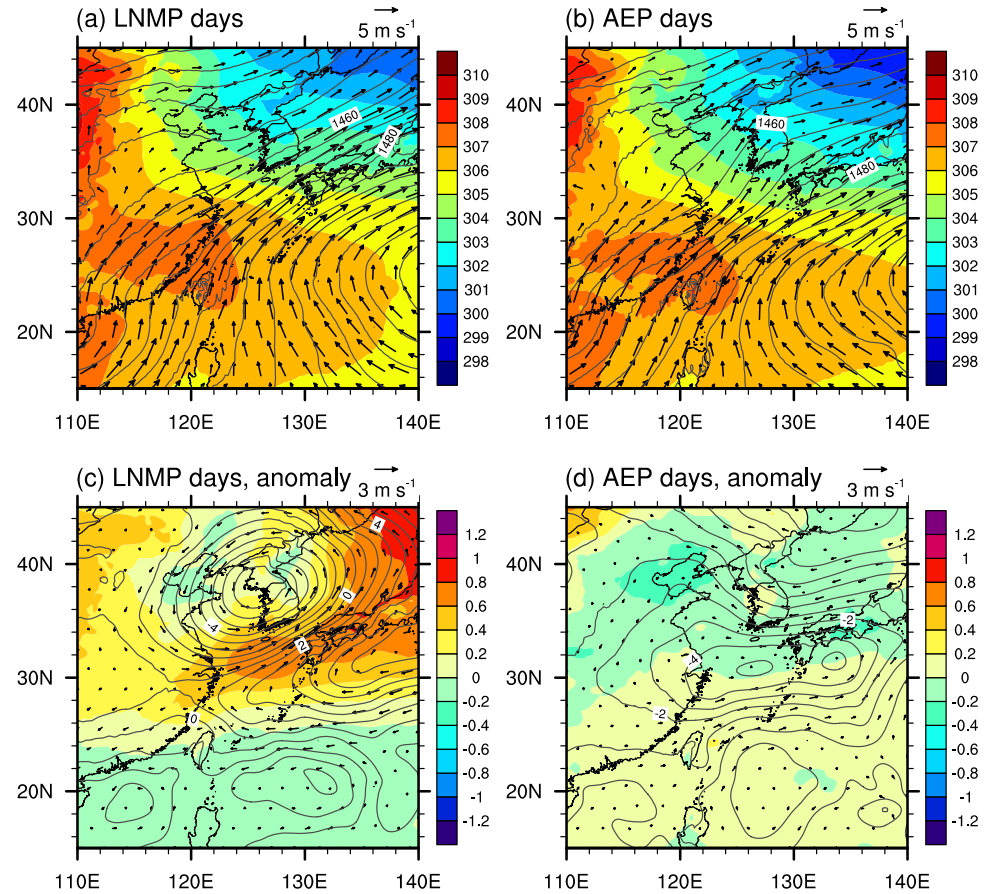


Large-scale low-level flows are known as an important factor for monsoonal precipitation in East Asia (Chen 2020). The low-level flows in the boundary layer have diurnal variation associated with inertial oscillation that occurs in response to the diurnal variation of the frictional effect of boundary layer mixing (Blackadar 1957), which is represented as clockwise rotation of the ageostrophic wind vector (Xue et al. 2018). To examine the role of the boundary layer inertial oscillation in the DVP in South Korea, the ageostrophic wind component is calculated by subtracting the geostrophic wind component from the total wind. To obtain the geostrophic wind component from the geopotential height field, a low-pass filter of Barnes (1964) is applied to the geopotential height field following Xu et al. (2017) and Xue et al. (2018) because the unfiltered field yields a noisy field of geostrophic wind component, especially for low levels. The constants in the Barnes filter are set to $g = 0.3$ and $c = 90,000$, which damps waves with 1000-km and 2000-km wavelengths by ~60% and ~15%,

respectively. Detailed information on the filtering method is provided in Xu et al. (2017).

The diurnal variations of the 925-hPa ageostrophic wind component anomaly and meridional wind component anomaly are presented in Fig. 8. On the LNMP days, the ageostrophic wind component anomaly in the East China Sea rotates clockwise, reflecting the boundary layer inertial oscillation. At 18 LST, when the frictional effect of the boundary layer is strong, the ageostrophic wind component anomaly has a direction opposite to the mean wind direction (Fig. 6a), weakening the low-level flow over the East China Sea toward South Korea. At 03 LST, the rotating ageostrophic wind component anomaly directs to South Korea. As a result, the low-level meridional wind component accelerates in the late night. These correspond to the diurnal monsoon variability. The enhanced supply of warm and moist air to the Changma front in the late night to morning, and the weakened monsoonal flow in the afternoon to evening decreases the

Fig. 6 Composite fields of 850-hPa geopotential height (gray contours, in 5-m intervals), equivalent potential temperature (color shades, K) and wind vector (arrows) for the (a) LNMP days and (b) AEP days and (c, d) their anomalies from all day means



precipitation during that time period on the LNMP days. On the AEP days, the clockwise rotation of ageostrophic wind component anomaly is also found over the East China Sea, but the amplitude of this inertial oscillation is relatively weak over latitudes higher than $\sim 30^{\circ}\text{N}$. This is because the amplitude of ageostrophic inertial oscillation is proportional to the geostrophic wind speed (Klein et al. 2016; Xue et al. 2018) and the geostrophic wind component is weak in the northern part of the East China Sea due to the loose pressure gradient there (Fig. 6b) on the AEP days. As a result, the nocturnal acceleration of meridional wind component does not significantly affect precipitation in South Korea.

Figure 9 shows how deeply the diurnal variation of meridional wind component is related to the DVP in South Korea. The time series of diurnal anomalies of precipitation in South Korea on the LNMP days is deeply correlated with the time series of diurnal anomalies of low-level meridional wind component over the northern part of the East China Sea and the south sea of the Korean Peninsula, with a maximum correlation coefficient of 0.49. This suggests that a large portion of the DVP on the LNMP days can be attributed to the diurnal monsoon variability represented by the nocturnal acceleration of meridional wind component. On the AEP days, however, the correlation is relatively weak,

indicating that diurnal monsoon variability is relatively less important for DVP on these days than on the LNMP days.

3.3.2 Diurnal variation of thermodynamic instability

The thermodynamic instability of atmosphere is diurnally modulated by vertically differential heating, and this can contribute to DVP. In clear regions, solar radiation heats the surface and destabilizes the low atmosphere in the daytime, contributing to the afternoon precipitation. On the other hand, in cloudy regions, daytime solar radiation stabilizes the atmosphere and suppresses daytime precipitation. In the nighttime, if clouds pre-exist, longwave radiative cooling at the cloud top increases the thermal lapse rate at the upper levels, which can enhance upper-level convection and hence late night-to-morning precipitation (Randall et al. 1991). Large-scale longwave radiative cooling can increase relative humidity and enhance the production of condensates in the nighttime, although this effect is known to be smaller in the mid-latitudes than in the tropics (Tao et al. 1996). The contributions of these mechanisms to DVP are different between the LNMP days and AEP days.

Figure 10a shows the diurnal variations of downward shortwave radiation at the surface averaged over the rain

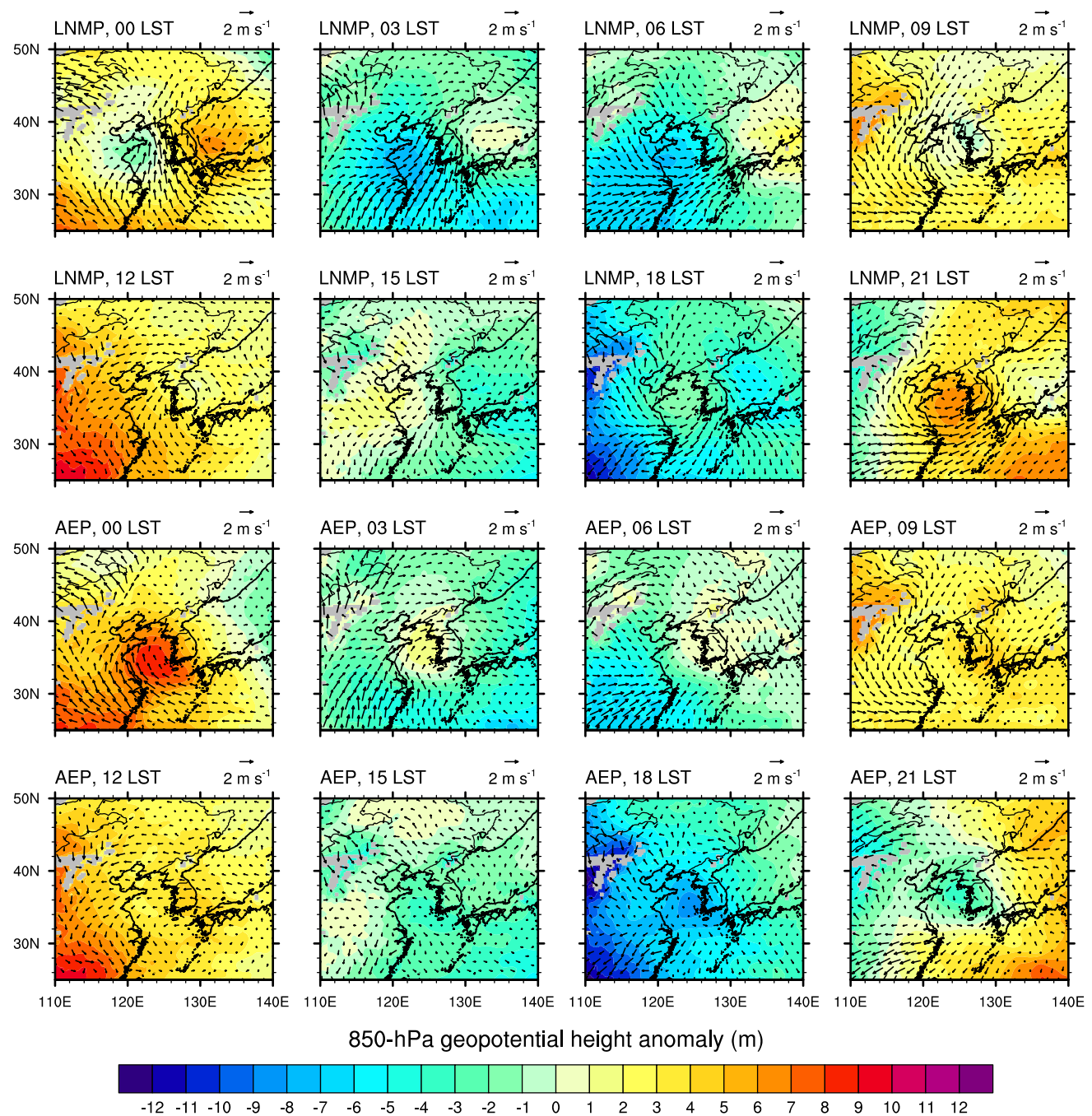


Fig. 7 Fields of 850-hPa geopotential height (color shades) and wind vector (arrows) at different times on the LNMP days (top two rows) and AEP days (bottom two rows). The variables are anomalies from the LNMP day mean and AEP day mean

gauge points on the two groups of rainy days. There are noticeable differences in the shortwave radiation from the morning to early afternoon between the LNMP days and AEP days. On the AEP days, the surface receives 20% more solar radiation at 06–15 LST than on the LNMP days, implying a larger role of surface heating in the DVP on these days. On the LNMP days, some clouds are sustained from

late night to daytime and block solar radiation and reduce thermodynamic instability, which can suppress afternoon convection and precipitation. Figure 11 shows the resultant differences in the diurnal variation of low-level thermodynamic instability between the LNMP days and AEP days. Compared to the LNMP days, the AEP days exhibit a higher diurnal variability of equivalent potential temperature

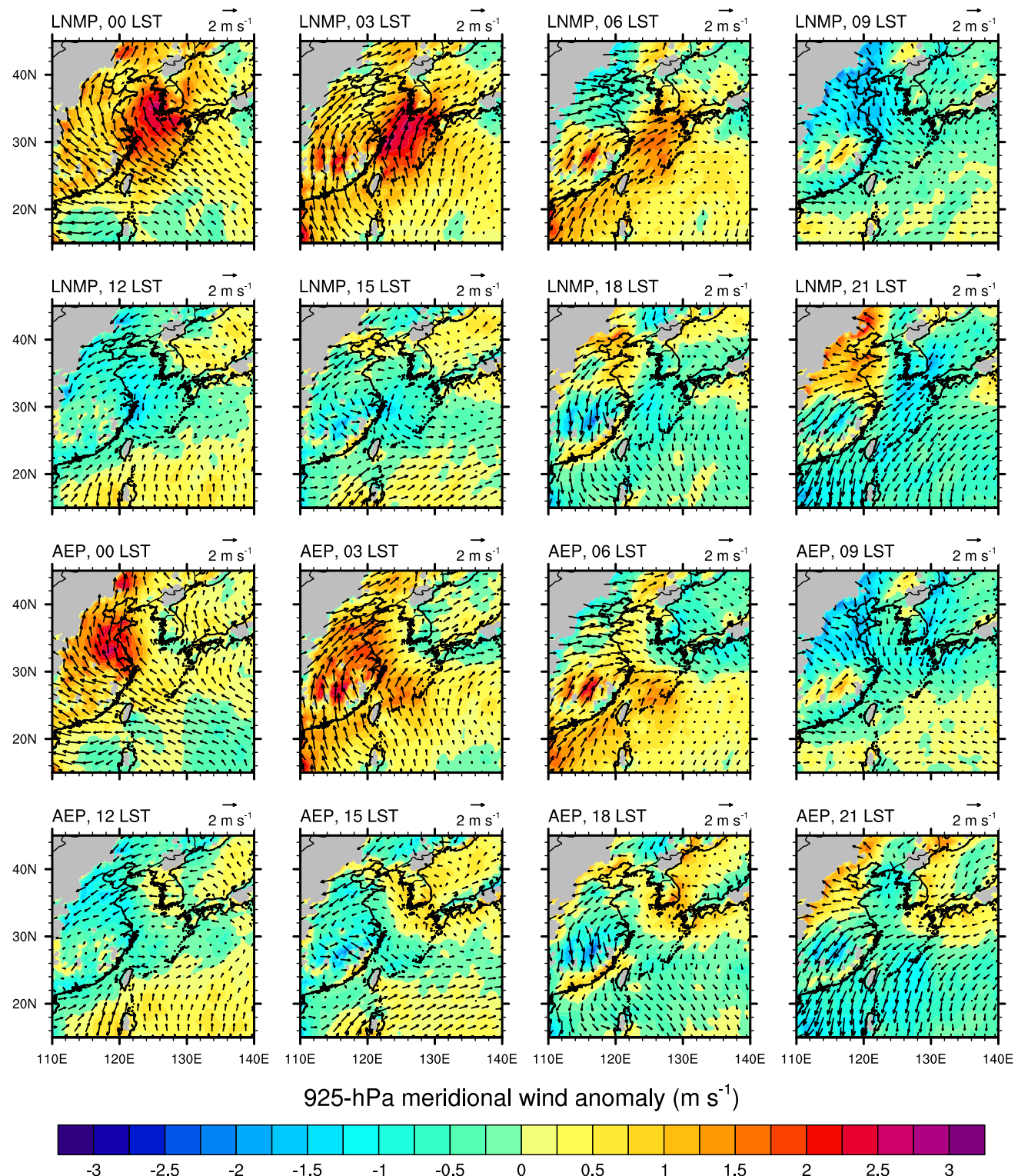


Fig. 8 Fields of 925-hPa meridional wind component (color shades) and ageostrophic wind vector (arrows) at different times on the LNMP days (top two rows) and AEP days (bottom two rows). The variables are anomalies from the LNMP day mean and AEP day mean

at the lowest levels, which reflects greater nighttime radiative cooling and daytime solar heating at the surface. The difference in equivalent potential temperature between 850

and 1000 hPa is 0.6 K smaller on the AEP days than on the LNMP days at 12 LST, indicating that the low atmosphere is thermodynamically less stable on the AEP days. This

Fig. 9 Fields of correlation coefficient between hourly precipitation amount averaged over all rain gauge points in South Korea and 925-hPa meridional wind component at each ERA5 grid point (color shades) on the (a) LNMP days and (b) AEP days. Both variables are diurnal anomalies from the daily mean. Only the statistically significant correlation coefficients are plotted (at the 99% confidence level). Fields of 925-hPa wind vector for the LNMP days and AEP days are anomalies from all day mean and represented by arrows

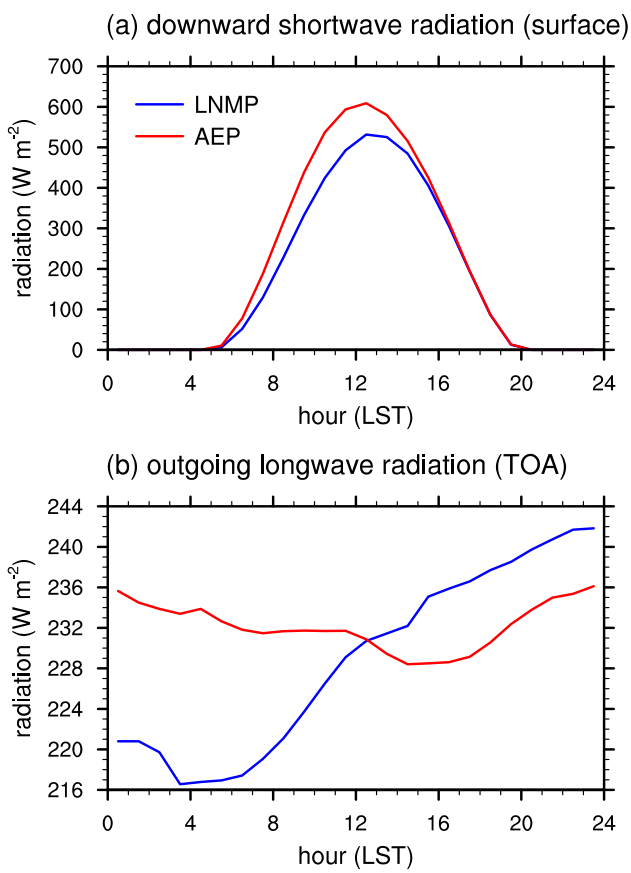
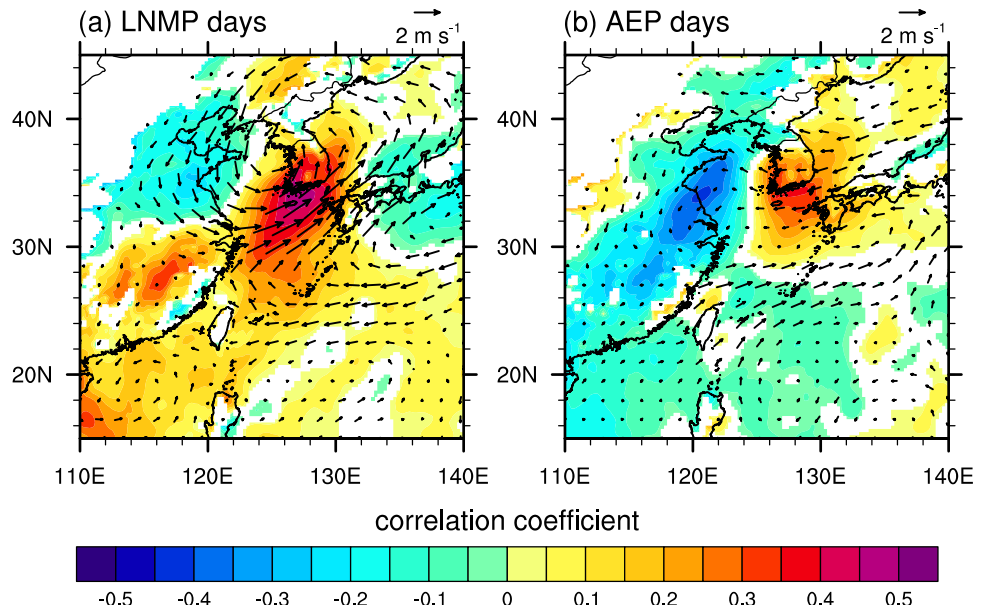


Fig. 10 Diurnal variations of (a) downward shortwave radiation at the surface and (b) outgoing longwave radiation at the top of the atmosphere averaged over all rain gauge points in South Korea on the LNMP days and AEP days

difference in thermodynamic conditions contributes to the relatively large (small) amount of afternoon precipitation on the AEP (LNMP) days.

Nighttime radiative cooling at the cloud top can enhance late night-to-morning precipitation on the LNMP days when clouds are likely to pre-exist. For a rigorous examination of the role of this mechanism in the DVP, cloud-resolving model simulations may be required because the destabilization of the upper troposphere by cloud top cooling can be immediately followed by the enhancement of convection that stabilizes the upper troposphere. In this study, however, it is examined only indirectly by presenting the features that could be brought by this mechanism. Figure 10b shows the diurnal variations of outgoing longwave radiation at the top of the atmosphere averaged over the rain gauge points. On the LNMP days, the outgoing longwave radiation is very small in the late night to morning, reflecting the existence and wide horizontal coverage of upper-level clouds. A drop of outgoing longwave radiation is found at 02–04 LST on the LNMP days, which may be partly attributed to the strengthening of upper-level convection and the consequent increase in the amount of upper-level hydrometeors. Figure 12a shows that large amounts of hydrometeors, mostly snow, exist in the upper troposphere at 00 LST and they increase during the late night until 06 LST on the LNMP days. The vertical extents of clouds do not change much diurnally, but the increase in upper-level snow amount enhances late night-to-morning precipitation. The upper-level clouds decrease considerably during the daytime, which may be partly attributed to upper-level stabilization by the absorption of solar radiation and to the diurnal variation of convective activity on the LNMP days caused by that of synoptic-scale forcing

Fig. 11 Vertical profiles of equivalent potential temperature averaged over all rain gauge points in South Korea at different times on the (a) LNMP days and (b) AEP days

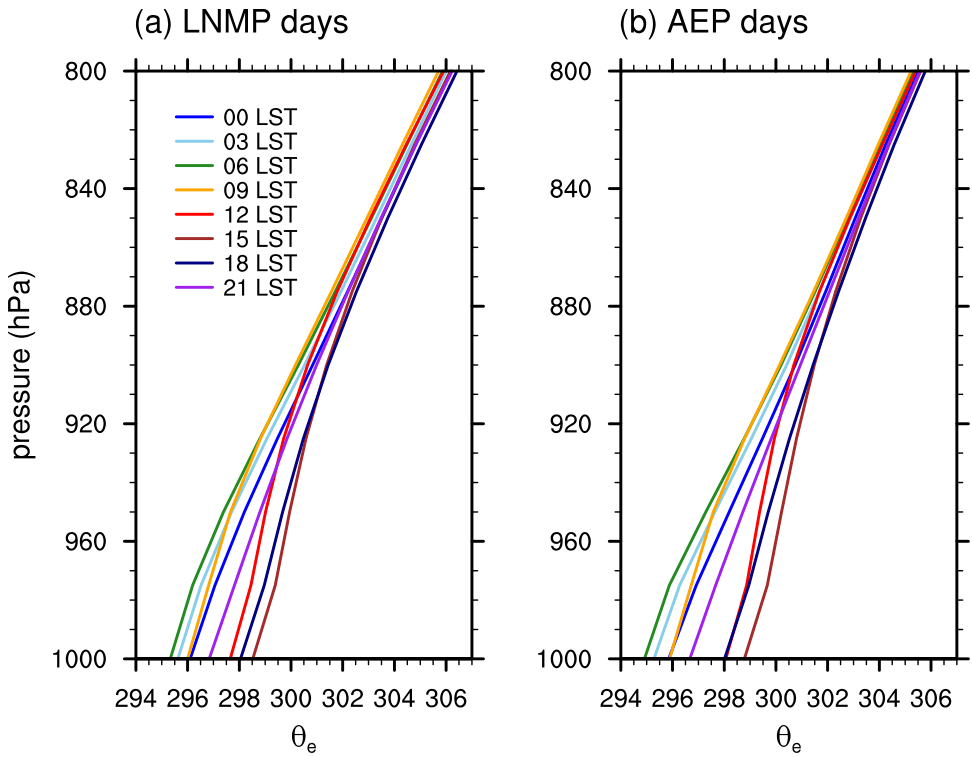
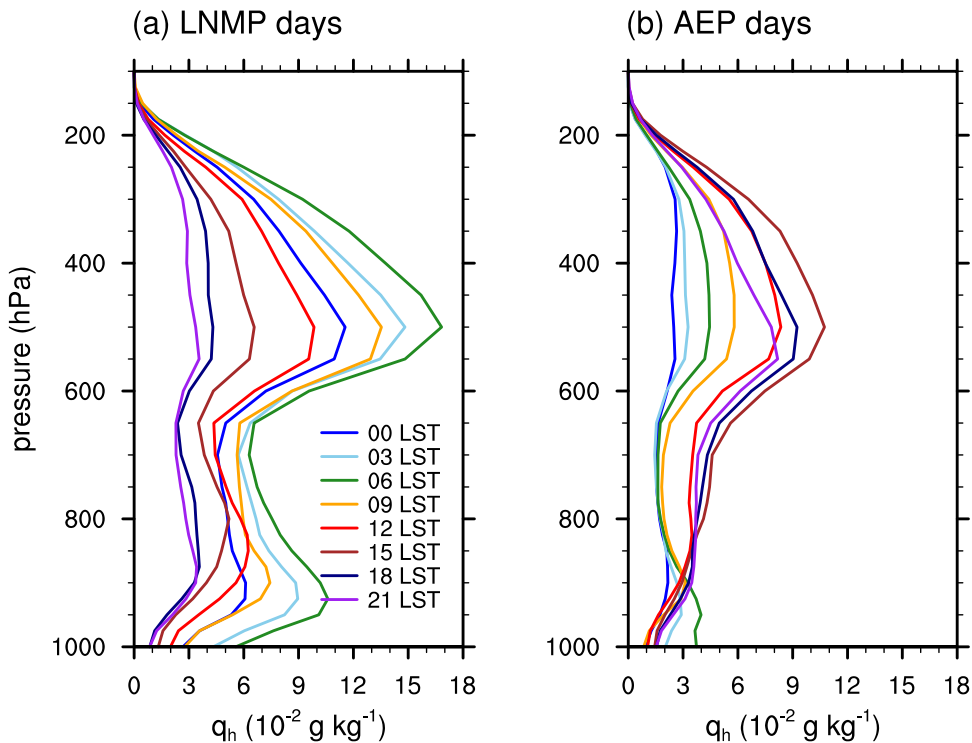


Fig. 12 Vertical profiles of total hydrometeor content averaged over all rain gauge points in South Korea at different times on the (a) LNMP days and (b) AEP days



(subsection 3.3.1). Both cloud cover and cloud top height overall decrease after 08 LST (not shown), which explains the increase in outgoing longwave radiation. On the AEP days, the vertical extents of clouds are as high as those

on the LNMP days (Fig. 12b), but the minimum outgoing longwave radiation is much greater than that on the LNMP days partly because of the smaller horizontal extents of the upper-level clouds (Fig. 10b).

3.3.3 Diurnal variation of local wind circulation

Another important mechanism for DVP is the diurnal variation of local wind circulation driven by horizontal differences in daytime heating and nighttime cooling of the surface. This mechanism is responsible for the different DVPs in different regions within South Korea. Because of the complex geography of this country, both land/sea breezes and mountain–plains solenoid significantly affect the local wind circulation.

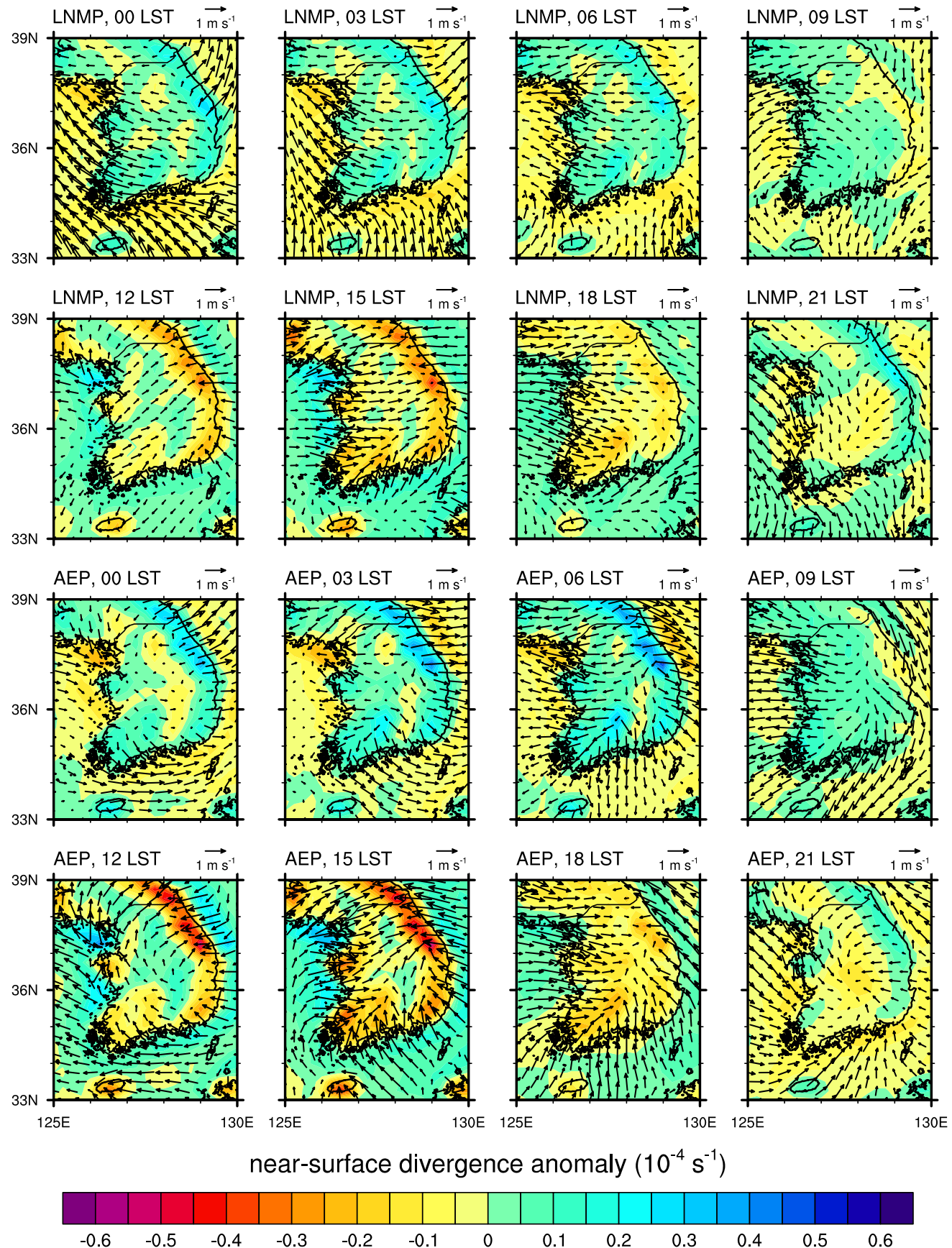
Figure 13 shows the diurnal variation of near-surface wind vector anomaly and its divergence on the LNMP days and AEP days. Because the skies are clearer from midnight to 15 LST on the AEP days than on the LNMP days, the AEP days exhibit a stronger diurnal variation of local wind circulation. On the AEP days, land breezes and downslope winds are prominent at 06 LST, and sea breezes and upslope winds dominate the country at 15 LST. As a result, strong near-surface divergence anomalies are found over the Taebaek Mountains, Sobaek Mountains, and Jeju Island at 06 LST, while strong near-surface convergence anomalies appear there at 15 LST. The strong convergence anomalies in the afternoon over these regions match well with the regions with large precipitation amounts on the AEP days (Fig. 5b). The convergence anomalies over the mountainous regions weaken as the evening arrives. Interestingly, at 21 LST, the inland regions exhibit relatively strong near-surface convergences compared to those in the mountainous regions and coastal regions. At this time, downslope winds develop, while land breezes do not develop yet in the western part of the country, generating a convergence zone over the inland regions. This explains the large amounts of precipitation in the inland regions on the AEP days (Fig. 5b) and the evening precipitation peak in the inland region between the Taebaek Mountains and Sobaek Mountains (east of the Sobaek Mountains) (Figs. 3a and 5d). In addition, a near-surface convergence anomaly is sustained over the south coastal region from 12 to 21 LST, enhancing precipitation there. In the late night to morning, the prevailing divergence anomalies suppress the precipitation during this time period on the AEP days.

On the LNMP days, the near-surface divergence anomalies in South Korea in the late night to morning are relatively weak compared to those on the AEP days due to the weaker radiative cooling of the surface under the high cloud cover. Rather, the convergence anomalies over the south sea of the country in the late night to early morning on the LNMP days are stronger than those on the AEP days, which are produced by the confrontation of the weak land breezes and enhanced low-level southerlies in the late night. This contributes to the late night-to-morning precipitation over the south coastal region on the LNMP days (Fig. 5a).

Figure 14 shows the correlation between the near-surface convergence anomaly and the DVP in South Korea. On the AEP days, the time series of diurnal anomalies of precipitation in South Korea is positively correlated with the time series of diurnal anomalies of near-surface convergence over most parts of the country. In particular, the Taebaek Mountains and south coastal region exhibit relatively high correlation coefficients, indicating large contributions of the near-surface convergences in the afternoon to evening over these regions to the afternoon-to-evening precipitation peak on the AEP days. On the LNMP days, however, negative or no correlations appear in most parts of the country. This suggests that the daytime convergence anomalies over land driven by the local wind circulation have no significant contributions to the DVP on the LNMP days. Rather, as mentioned above, the near-surface convergence over the south sea of the country in the late night contributes to the late night precipitation on the LNMP days.

To further investigate the effects of local wind circulation on the diurnal variation of convective activity, the diurnal variation of vertical velocity anomaly together with that of equivalent potential temperature anomaly is presented on the longitude–pressure cross section along the latitude 37.5°N that crosses the Taebaek Mountains where the diurnal variability of near-surface convergence is maximized (Fig. 15). On the AEP days, a strong upward velocity anomaly appears during ~ 12–15 LST over the eastern slope of the Taebaek Mountains due to the upslope winds driven by the large thermal contrast between the mountains and the sea in the east. The upward velocity anomaly reaches the upper troposphere at ~ 18 LST, which indicates the development of deep convection. In the western part of the country, the development of upward velocity anomaly driven by the sea breezes is relatively late compared to that in the eastern slope of the Taebaek Mountains. At 18 LST, upward velocity anomalies cover almost all of the land at this latitude and affect the precipitation there. During 03–06 LST, relatively weak upward velocity anomalies appear over the west and east coastal regions, while most parts of the land exhibit downward velocity anomalies that suppress the late night-to-morning precipitation on the AEP days.

On the LNMP days, a large-scale convective system approaches from the west to the land in the late night. The convective system is vertically well developed and has a much larger horizontal scale than that on the AEP days. Although a downward velocity anomaly develops over the eastern slope of the Taebaek Mountains during 00–06 LST, this system crawls over it. The afternoon upward velocity anomalies over the land on the LNMP days are not only relatively weak but also confined within the low levels compared to those on the AEP days.



◀Fig. 13 Fields of 10-m wind vector (arrows) and its divergence (color shades) at different times on the LNMP days (top two rows) and AEP days (bottom two rows). The variables are anomalies from the LNMP day mean and AEP day mean

4 Summary and conclusions

Using 10-yr nationwide rain gauge data, the characteristics of diurnal variation of June–July precipitation in South Korea and possible mechanisms were examined. The summertime DVP in South Korea has two peaks: a primary peak at 05–08 LST and a secondary peak at 16–18 LST. For the morning peak of precipitation amount, the contribution of precipitation intensity is larger than the contribution of precipitation frequency, while the precipitation frequency contributes slightly more to the late afternoon peak. Spatially, afternoon-to-evening peaks (14–22 LST) appear in the mountainous regions and the south coastal region, and late night-to-morning peaks (02–10 LST) appear in the west and east coastal regions and the western inland regions west of the mountainous regions. Rainy days are divided into the LNMP days and AEP days according to the peak time of precipitation, and these two groups of rainy days have clearly different characteristics of DVP and relevant mechanisms.

The LNMP days are characterized by enhanced large-scale low-level southwesterlies toward South Korea and resultant large-scale and heavy precipitation. The low pressure anomaly over the Yellow Sea in the late night, the nocturnal acceleration of low-level monsoonal southerlies driven by the boundary layer inertial oscillation, and the cloud top radiative cooling are responsible for the precipitation peak on the LNMP days. The AEP days are characterized by relatively weak synoptic forcing for precipitation. The destabilization of the low atmosphere due to daytime surface heating and the local wind circulations that cause strong near-surface convergence anomalies over the mountainous regions in the afternoon and over the inland region in the evening are important mechanisms for DVP on the AEP days.

Using precipitation data from a dense network of rain gauges, this study reveals detailed spatiotemporal

characteristics of DVP in South Korea and their relations to the complex geographical features of the country, which previous studies using data from a small number of rain gauges could not examine. Also, this study shows how the diurnal variations of synoptic-scale circulation, thermodynamic instability, and local wind circulation contribute to DVP in South Korea. Such comprehensive investigation on the various possible mechanisms that are responsible for DVP in South Korea has never been done before.

In this study, the recent 10-year period is selected as the study period to use data from a denser network of rain gauges than before. The characteristics of DVPs in prior decades and their differences from the DVP in the recent years deserve future investigation because the interdecadal variability of the East Asian summer monsoon (Zhang et al. 2018) as well as the climate change may have had some effects on the summertime DVP in South Korea.

Although possible mechanisms for the DVP in South Korea are investigated in this study, the relative importance of these mechanisms is not revealed. Understanding of DVP in South Korea will be deepened if quantitative comparisons among the contributions of different mechanisms to the DVP are provided by numerical modeling studies in the future.

Acknowledgements The authors thank the Korea Meteorological Administration for providing the rain gauge data.

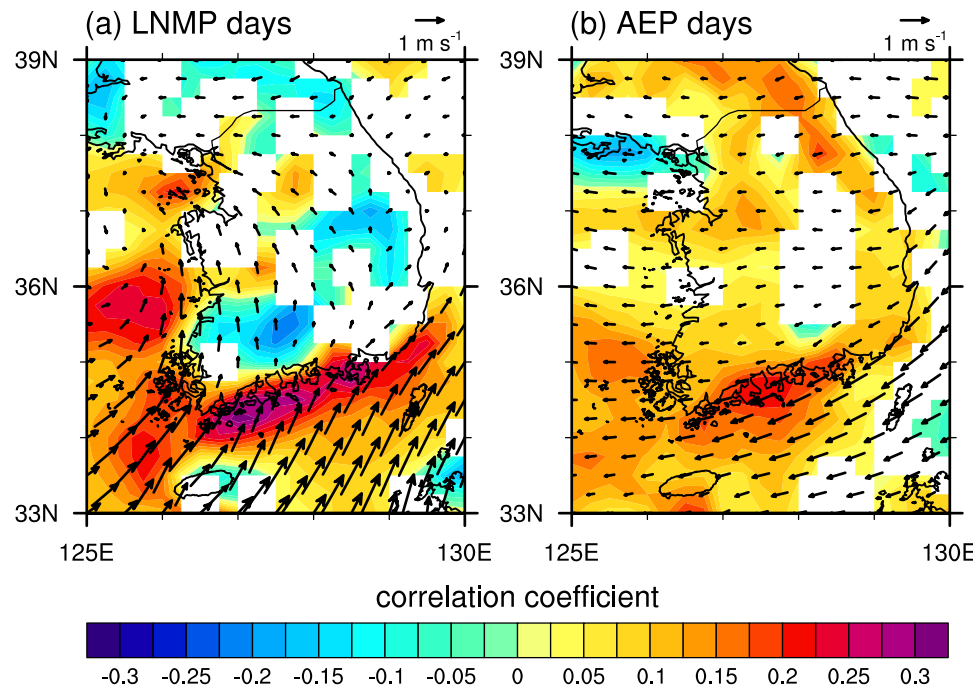
Author contributions Jong-Jin Baik designed this study. Han-Gyul Jin performed the data analysis and visualization. All authors discussed the results. Han-Gyul Jin wrote the original draft. Hyunho Lee and Jong-Jin Baik reviewed and edited the manuscript. All authors read and approved the final version of the manuscript.

Funding This work was supported by the National Research Foundation of Korea (NRF) under grants 2019R1A6A1A10073437 and 2021R1A2C1007044.

Data availability The rain gauge data were provided by the Korea Meteorological Administration. The ERA5 data were downloaded from the Copernicus Climate Change Service (C3S) Climate Data Store (CDS).

Code availability The codes used for analyses in this study can be obtained from the corresponding author if necessary.

Fig. 14 Fields of correlation coefficient between hourly precipitation amount averaged over all rain gauge points in South Korea and near-surface convergence at each ERA5 grid point (color shades) on the (a) LNMP days and (b) AEP days. Both variables are diurnal anomalies from the daily mean. Only the statistically significant correlation coefficients are plotted (at the 99% confidence level). Fields of 10-m wind vector for the LNMP days and AEP days are anomalies from all day mean and represented by arrows



Declarations

Conflict of interest We declare no conflict of interest.

Ethics approval Not applicable.

Consent to participate Not applicable.

Consent for publication Not applicable.

References

- Barnes SL (1964) A technique for maximizing details in numerical weather map analysis. *J Appl Meteorol* 3:396–409
- Blackadar AK (1957) Boundary layer wind maxima and their significance for the growth of nocturnal inversions. *Bull Amer Meteorol Soc* 38:283–290
- Chen G (2020) Diurnal cycle of the Asian summer monsoon: Air pump of the second kind. *J Clim* 33:1747–1775
- Fujibe F (1988) Diurnal variations of precipitation and thunderstorm frequency in Japan in the warm season. *Pap Meteorol Geophys* 39:79–94
- Hersbach H, Bell B, Berrisford P, Hirahara S, Horányi A, Muñoz-Sabater J, Nicolas J, Peubey C, Radu R, Schepers D, Simmons A, Soci C, Abdalla S, Abellán X, Balsamo G, Bechtold P, Biavati G, Bidlot J, Bonavita M, Chiara G, Dahlgren P, Dee D, Diamantakis M, Dragani R, Flemming J, Forbes R, Fuentes M, Geer A, Haimberger L, Healy S, Hogan RJ, Hólm E, Janisková M, Keeley S, Laloyaux P, Lopez P, Lupu C, Radnoti G, Rosnay P, Rozum I, Vamborg F, Villaume S, Thépaut J-N (2020) The ERA5 global reanalysis. *Q J R Meteorol Soc* 146:1999–2049
- Huang L, Mo Z, Liu L, Zeng Z, Chen J, Xiong S, He H (2021) Evaluation of hourly PWV products derived from ERA5 and MERRA-2 over the Tibetan Plateau using ground-based GNSS observations by two enhanced models. *Earth Space Sci* 8:e2020EA001516
- Jung H-S, Lim G-H, Oh J-H (2001) Interpretation of the transient variations in the time series of precipitation amounts in Seoul, Korea. Part I: Diurnal variation. *J Clim* 14:2989–3004
- Kim K, Eom D-Y, Lee D-K, Kuo Y-H (2010) Diurnal variation of simulated 2007 summer precipitation over South Korea in a real-time forecast model system. *Asia-Pac J Atmos Sci* 46:505–512
- Klein PM, Hu X-M, Shapiro A, Xue M (2016) Linkages between boundary-layer structure and the development of nocturnal low-level jets in central Oklahoma. *Bound-Lay Meteorol* 158:383–408
- Li R, Wang K, Qi D (2018) Validating the Integrated Multisatellite Retrievals for Global Precipitation Measurement in terms of diurnal variability with hourly gauge observations collected at 50,000 stations in China. *J Geophys Res: Atmos* 123:10423–10442
- Li Z, Yu W, Li T, Murty VSN, Tangang F (2013) Bimodal character of cyclone climatology in the Bay of Bengal modulated by monsoon seasonal cycle. *J Clim* 26:1033–1046
- Lim G-H, Kwon H-J (1998) Diurnal variation of precipitations over South Korea and its implication. *J Korean Meteorol Soc* 34:222–237
- Oki T, Musiakie K (1994) Seasonal change of the diurnal cycle of precipitation over Japan and Malaysia. *J Appl Meteorol Climatol* 33:1445–1463
- Qian W, Kang H-S, Lee D-K (2002) Distribution of seasonal rainfall in the East Asian monsoon region. *Theor Appl Climatol* 73:151–168
- Ramage CS (1952) Diurnal variation of summer rainfall over east China, Korea, and Japan. *J Atmos Sci* 9:83–86
- Randall DA, Harshvardhan H, Dazlich DA (1991) Diurnal variability of the hydrologic cycle in a general circulation model. *J Atmos Sci* 48:40–62
- Roh J-W, Lee Y-H, Nam J-E, Chung K-Y (2012) Diurnal variations of summertime precipitation in South Korea in 2009 using precipitation reanalysis data. *SOLA* 8:155–159
- Song Z, Zhang J (2020) Diurnal variations of summer precipitation linking to the topographical conditions over the Beijing-Tianjin-Hebei region. *Sci Rep* 10:9701
- Tao W-K, Lang S, Simpson J, Sui C-H, Ferrier B, Chou M-D (1996) Mechanisms of cloud-radiation interaction in the tropics and mid-latitudes. *J Atmos Sci* 53:2624–2651

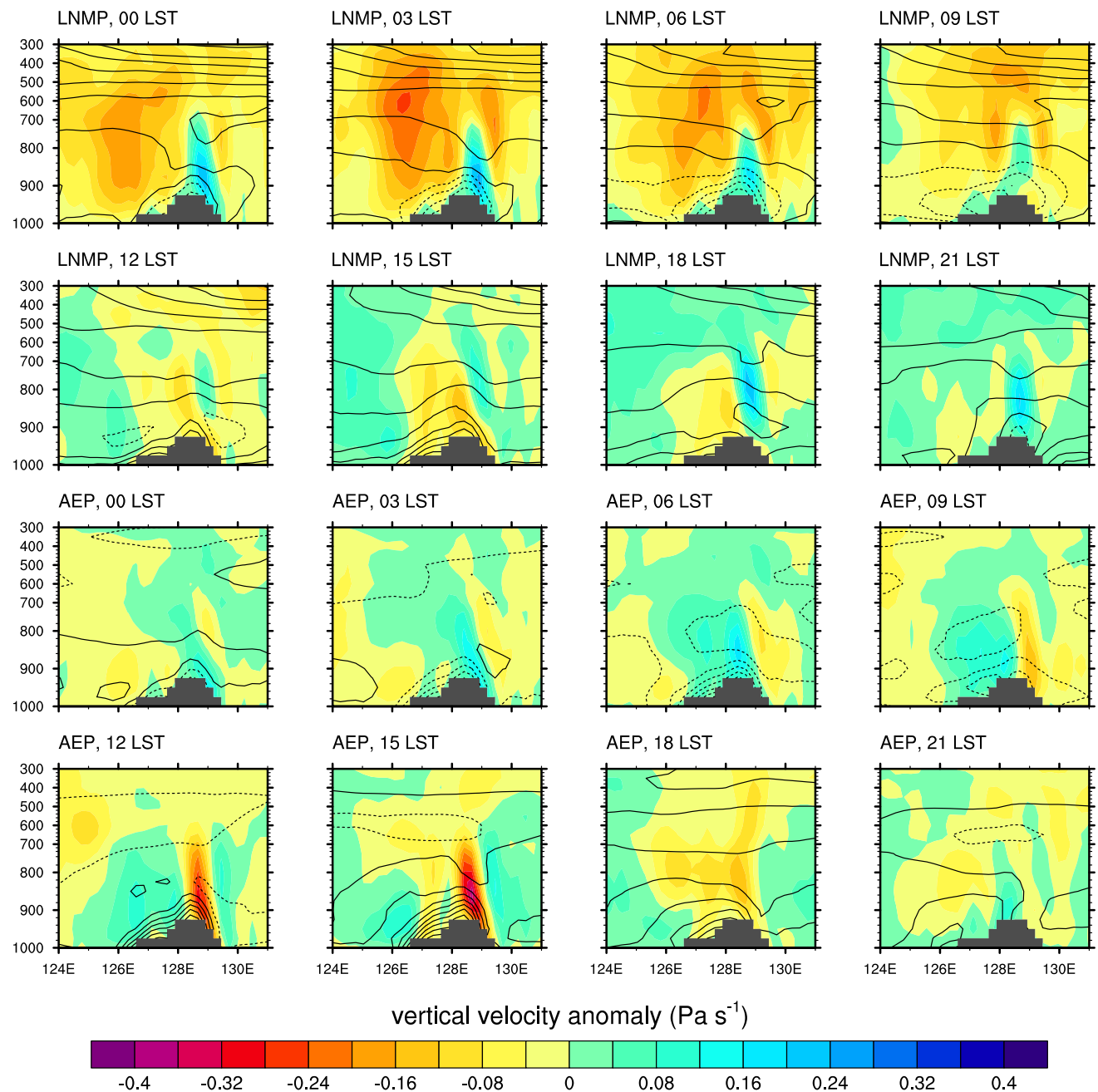


Fig. 15 Longitude–pressure cross sections of vertical velocity (color shades) and equivalent potential temperature (solid and dashed black contours, in 0.4-K intervals) along the latitude of 37.5°N at different times on the LNMP days (top two rows) and AEP days (bottom two rows). The variables are anomalies from the LNMP day mean and AEP day mean. The solid and dashed contours indicate positive and negative values, respectively

- Xu X, Xue M, Wang Y, Huang H (2017) Mechanisms of secondary convection within a Mei-Yu frontal mesoscale convective system in eastern China. *J Geophys Res: Atmos* 122:47–64
- Xue M, Luo X, Zhu K, Sun Z, Fei J (2018) The controlling role of boundary layer inertial oscillations in Meiyu frontal precipitation and its diurnal cycles over China. *J Geophys Res: Atmos* 123:5090–5115

- Yu R, Zhou T, Xiong A, Zhu Y, Li J (2007) Diurnal variations of summer precipitation over contiguous China. *Geophys Res Lett* 34:L01704
- Yuan W, Li J, Chen H, Yu R (2012a) Intercomparison of summer rainfall diurnal features between station rain gauge data and TRMM 3B42 product over central eastern China. *Int J Climatol* 32:1690–1696

- Yuan W, Yu R, Zhang M, Lin W, Chen H, Li J (2012b) Regimes of diurnal variation of summer rainfall over subtropical East Asia. *J Clim* 25:3307–3320
- Zhang Z, Sun X, Yang X-Q (2018) Understanding of the interdecadal variability of East Asian summer monsoon precipitation: Joint influence of three oceanic signals. *J Clim* 31:5485–5506

Publisher's note Springer Nature remains neutral with regard to jurisdictional claims in published maps and institutional affiliations.